LATVIAN JOURNAL OF PHYSICS AND TECHNICAL SCIENCES
2017, N 4

DOI: 10.1515/lpts-2017-0024

MEASUREMENTS OF WAVE POWER IN WAVE ENERGY CONVERTER EFFECTIVENESS EVALUATION

J. Berins[1], J. Berins[2], A. Kalnacs[3]
[1] Faculty of Automation and Computer Engineering, Riga Technical University
1 Kalku Str., Riga, LV-1658, LATVIA
[2] Faculty of Power and Electrical Engineering, Riga Technical University
1 Kalku Str., Riga, LV-1658, LATVIA
[3]Institute of Physical Energetics
11 Krivu Str., Riga, LV-1006, LATVIA

The article is devoted to the technical solution of alternative budget measuring equipment of the water surface gravity wave oscillation and the theoretical justification of the calculated oscillation power. This solution combines technologies such as lasers, WEB-camera image digital processing, interpolation of defined function at irregular intervals, volatility of discrete Fourier transformation for calculating the spectrum.

Keywords: *discrete Fourier transformation, effectiveness, function interpolation, image processing, laser beam, spectrum, wave energy converter, wave height, wave power.*

1. INTRODUCTION

In the project "Operation Research of a Twisting and Rotating Wave Energy Conversion Plant", the objective was to assess the efficiency of dynamic systems of the energy receiver and converters in an environment such as waves. Resulting analysis showed that this could be achieved through specific measurement of time and space that fully characterised the environment without destroying it; it was both complex and at the same time within the project budget. This project phase resulted in technical measuring equipment for which there were other applications, such as level sensors of converters for adequate management development to ensure active wave energy capture systems. The draft of the proposed technical solution is based on the conservation of energy and the dynamic potential and kinetic energy balance of the surface wave in the gravitational field. Fixing the water surface elevation changes, characterised by the fluid potential energy during the time of change; it is possible to quantify the corresponding kinetic energy changes as well as the total energy of the system. It is a dynamic system so that the process of various measuring steps necessitates automation.

2. LASER MEASURE STRUCTURE

As a solution we used a laser height gauge, the web camera (the camera) image projected on the screen – float (at a certain angle) by the incident laser beam (beam) created light contrast "point" (Fig. 1). If the float is placed in the liquid, which is subject to wave type fluctuations, the vertical distance from the ray source will change and the image on camera will show the point horizontal offset. Fixing certain parameters in such a system, it is possible to solve the problem in an alternative way: measuring the point shift, it is possible to calculate the absolute distance of the surface or the relative deviation from the steady state.

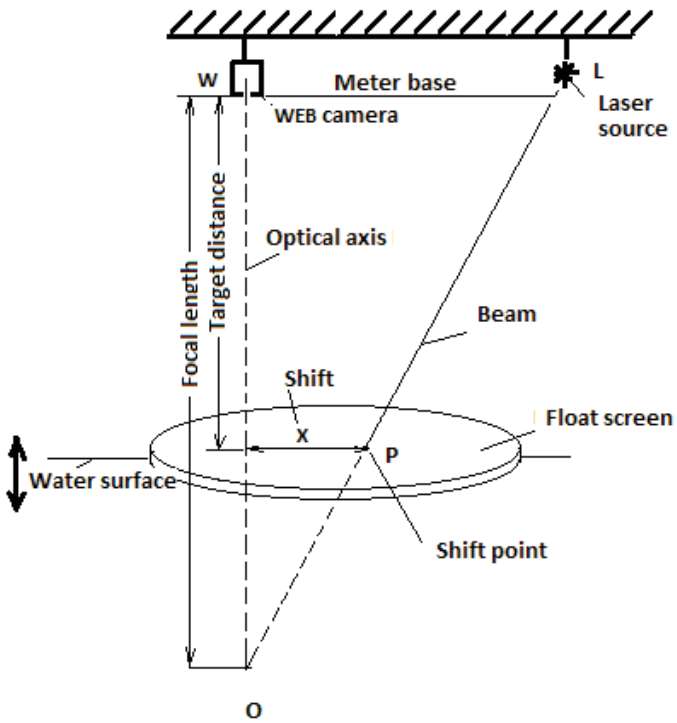

Fig. 1. Laser meter scheme.

This solution is functional and simple. In laboratory conditions, it promises to be sufficiently accurate.

3. OPTICAL SHEMATIC

Optical scheme (Fig. 2) space has two measurement dimensions consisting of vertically downward right-angled triangle whose hypotenuse LO is formed by a laser beam. Shorter cathetus WL with a narrow angle near the apex is formed by ray source L and camera W, whose lens centre is placed at the apex of the right-angled triangle. The central optical axis (the "axis") is WO. The straight edge of the camera centre to beam WL is base distance from camera to the laser source.

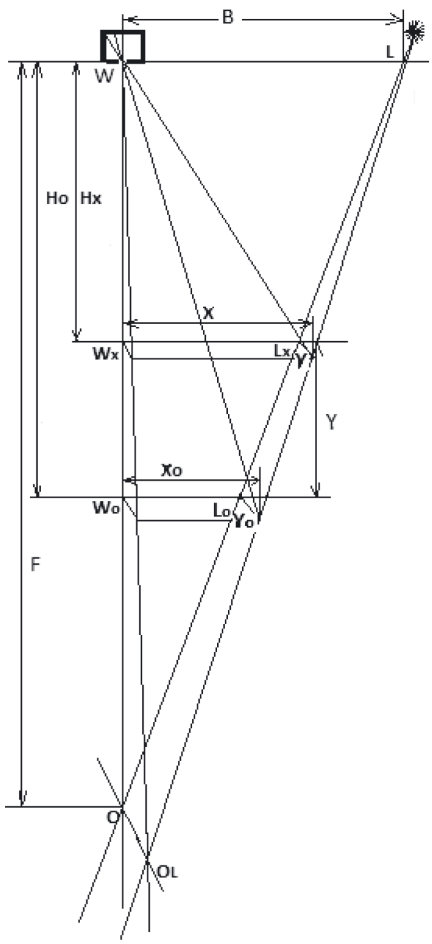

Fig. 2. Laser measure optical schematic.

The third dimension is used in beam LO shift OO_L from the measurement plane control and the vertical distance correction, if necessary. Thus, the float vertical distance between the triangle WLO apex O is expressed by two similar triangles W_0L_0O and WLO side ratios (Formula 1). In gauge terms, its looks like (Formula 2):

$$\frac{WO}{WL} = \frac{WxO}{WxLx}, \tag{1}$$

$$F - H_X = \frac{F}{B} \cdot X, \tag{2}$$

where H_x – the distance between the camera and the water level;

F – laser gauge focal distance;

B – laser gauge base distance;

X – laser beam shift from optical axis on float screen in millimetre.

The elevation Y measurement from zero water level *Wo*:

$$Y = H_0 - F \cdot (1 - \frac{X}{B}) \tag{3}$$

where, H_0 – the distance between the camera and the zero (no waves) water level *Wo*.

4. PIXEL LINEAR SIZE PROBLEM

The picture and images in the camera consist of pixels (dots). In an ordinary camera, there are 640x480 pixels. This is known as the standard VGA image resolution. Evaluation of the distance between two points in the camera image is not possible to detect in a different way than in these units. At the same time, it should be taken into account that the pixel is an angular unit. Every distance from camera corresponds to a different pixel linear dimension. In household applications, this is not critical, but in this case, it is necessary to know the camera pixel linear dimensions and to follow the changes in different distances from the camera lens (lens centre W). This means that given that the camera axis coordinates of the images in the camera are $x = 320$; $y = 240$, connection (3) expressing straight shift edge X in its linear dimensions has observable shift point coordinates. Thus, we obtain:

$$X = (x - 320) \cdot p_{X0} \cdot (\frac{1 + (x - x_0)}{H_0}), \tag{4}$$

where x – laser beam shift camera image from optical axis on float screen in pixels on the water level;

x_0 – the same on zero water level *Wo*;

p_{x0} – the pixel linear horizontal size at level H_0.

5. CALIBRATION

Constructive differences of various cameras and even one manufacturer's camera model or the influence of shifts can vary the pixel corresponding linear dimensions. After production the base measurement of B (cut-off) sizes may vary as the beam angle relative to the camera's optical axis can also vary. In this case, we chose a solution where in the manufacture of the equipment mechanical parts precision was not important. Numerical constants, which are necessary for processing the results of measurements, are obtained by calibrating equipment under laboratory conditions. The numerical values of linear distance are fixed in laboratory conditions. Distance Y and the shift X are calculated in (3) and (4). Unknown values are B and $p_{X0.}$ To obtain the determined solution, we need two independent equation systems, which means that it is necessary to fix system parameters in 2 different distance measurements.

A technical solution is that the beams and the optical axis angle depend on measuring conditions as soon as focal length F is variable and this measurement ad-

justment is made at the beginning of each measurement session, recording the shift from X_0 at a distance of H_0 (zero water level W_0).

The camera image has a fixed coordinate's window whose shift point should "hit". This is done to reduce image processing time and reduce the glare of different types of noise in the system.

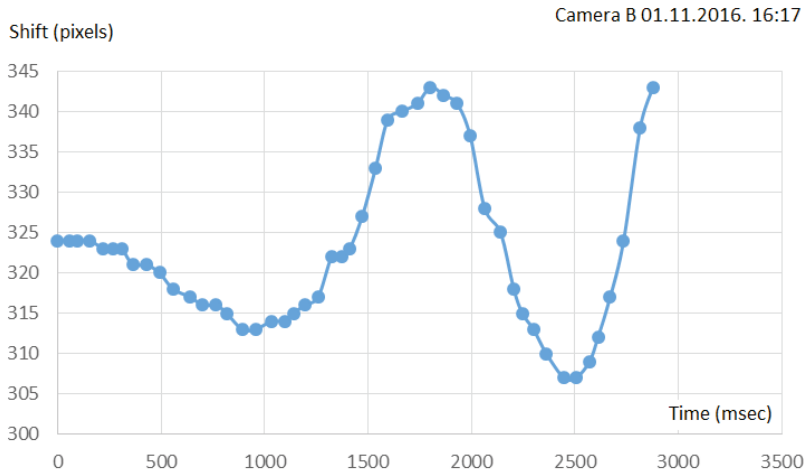

Fig.3. Graphical representation of B camera source data example.

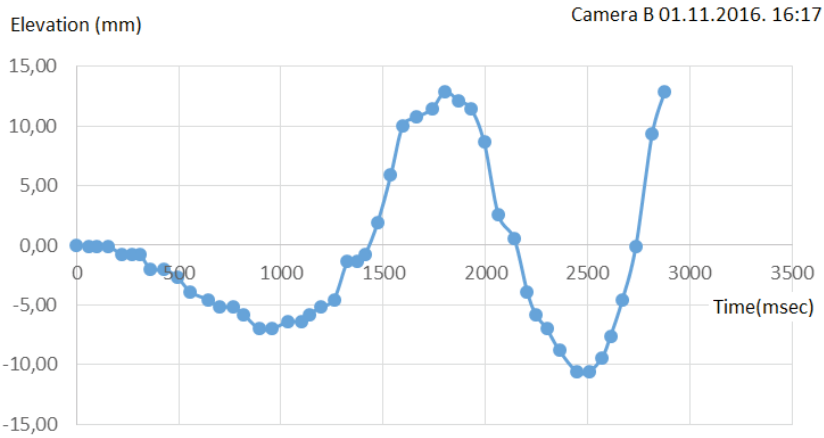

Fig. 4. Processed source data P_{X0} = 0.31mm B = 166.17mm.

6. MEASUREMENT PROCESSING

In measurement processing, we started with image processing: average shift point coordinate calculation, or the centre of the gravity coordinates and their fixation (in pixels) of the result file were synchronised with the time of the relative and absolute measurement of experimental sessions (in microseconds). As a result, we obtained source data. Example of source data sequence is shown in Fig. 3.

These data sequences are sufficient to be able to draw conclusions about waveform levels or offsets, but not "convenient" for the use of different analysis tools, further analysis of volatility, including components of the energy evaluation. The problem is the fact that in the processing of the data, we chose a universal computer, which runs the OS MS Windows 7. It has a number of advantages: user interface, device driver (connection interfaces and management programs), wide transmission spectrum of possibilities, data processing, storage and storage options. However, at the same time the prior complex process breaks in this case do not guarantee equal intervals between measurements, which leads to the next processing step based on intermittent time interval data replacement with as close as possible and smooth data substitution function $f = z\ (t)$, which provides realistic function values at any point in time.

7. INTERPOLATION SEGMENT AND INTERPOLATION WINDOW

Variable interpolation problem solutions were widely used in the past. There are a whole range of mathematical tools to solve this problem. The problem is the great number of variable defined points (several thousand). We introduced the "interpolation window" (Fig 5) and "interpolation segment" concepts. The interpolation segment has a final number of sequential time series data ($t_i\, Y_i$,) which are the subject of further analysis. The interpolation window has fixed number N of interpolation segment data, which allows using polynomial interpolation to get smooth curve approximation for incoming data. The interpolation process is carried out in two stages. In the first phase, using regression analysis with Excel LINEST array function polynomial modification, interpolation window "slides" (Fig. 5) over the interpolation segment. The N-th order polynomial coefficient value vector $K_{i,1}$: $K_{i,N+1}$ is calculated for substitution function expression for each window (5).

$$K_{i,1} : K_{i,N+1} = LINEST\left(Y_i : Y_{i+N}, t_i : t_{i+N}, pol\_order = N\right), \tag{5}$$

where Y_i:Y_{i+N} current interpolation window data set;
t_i:t_{i+N} current interpolation window time set.

The interpolation window is shifted by one step *(i+1)* and the polynomial coefficient calculations are repeated until the entire interpolation segment is thus treated ($i=1, \ldots, i_{max-N+1}$). The next step is to define a regular iteration step value Δt, choice of its number j_{max} and the selection of corresponding coefficient vector from an array of choice of features for substitution function $z\ (t_j)$ value calculation. To determine the irregular time interval, which corresponds to the current time t_j iteration value, $z(t_j)$ – function (8) built-in Excel tool *MATCH* based selective filter is used (6). For the $K_{i,1}$:$K_{i,N+1}$ vector addressing in the polynomial coefficient array an indirect addressing function *INDIRECT* (7) is used.

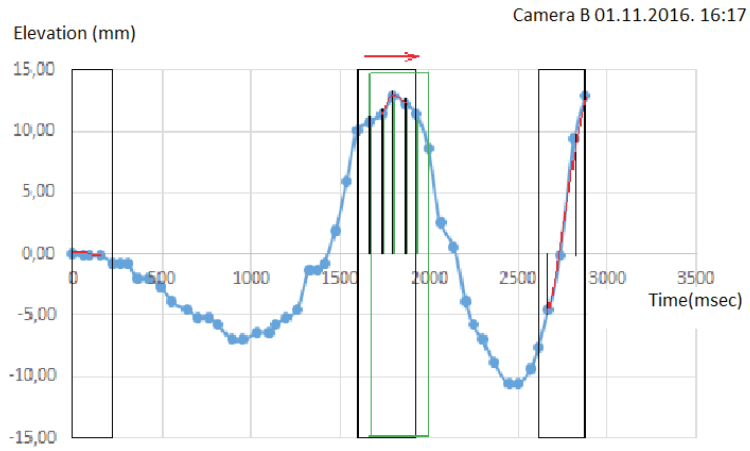

Fig. 5. Example of segment interpolated function with a sliding interpolation window.

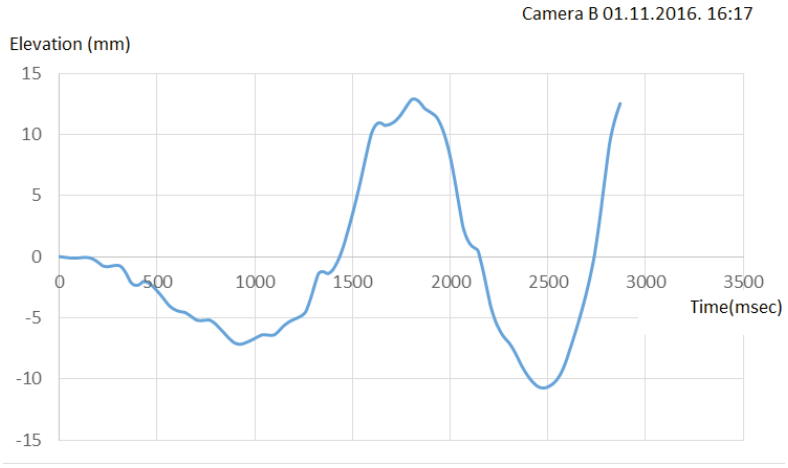

Fig. 6. Example of a smooth segment interpolated function with a regular iteration step Δt =7ms.

$$m = MATCH\left(t_j, t_i : t_{i\max}\right) \tag{6}$$

$$K_{j,1} : K_{j,N+1} = INDIRECT(array\ of\ coeficients[1:N, i:(i_{\max} - N + 1)], (m + D_m)), \tag{7}$$

where m – specific time interval fit number;

D_m – interpolation window interval shift for prevention curve distortions on interval borders.

As a result, we can obtain data substitution values (8) in any point of interpolation segment time

$$z(tj) = K_{j,1} \cdot t^N + K_{j,2} \cdot t^{N-1} + \ldots + K_{j,N} \cdot t + K_{j,N+1}, \tag{8}$$

for $j=1, \ldots, j_{max}$

8. DISCRETE FOURIER TRANSFORMATION

The next step in our wave analysis is irregular and unlinear oscillation split into various frequency sine wave components (9), [1].

The transformation result is a complex variable function (9) providing information about the relative contribution to the wave by each discrete frequency $k \cdot \Delta f$, for $j_{max}/2$ number of frequencies (regarding Nyquist criterion).

$$F(k \cdot \Delta f) = \sum_{j-1=0}^{j\,\max-1} z(j \cdot \Delta t) \cdot e^{-i(2\pi k \Delta f)\cdot(j-1)\Delta t}, \tag{9}$$

for k= 0, 1, 2, ...,j_{max-1}.

where k – discrete sine wave frequency number;

Δf – frequency resolution;

T – total sampling time or interpolation segment;

J_{max} – total number of discrete data points taken for analysis;

Δt – sampling time step value.

To obtain adequate results, we have to reduce unphysical error in the FFT called leakage. It is subject to follow certain conditions [1].

1. In principle, if an infinite number of discrete data points are taken, leakage would not be a problem. However, any real data acquisition system performing FFTs uses a finite number of discrete data points (in our case around 1000 points);
2. Time domain segment T for FFT application must be at least three oscillation periods (in practice at least 4 oscillation periods are used).
3.

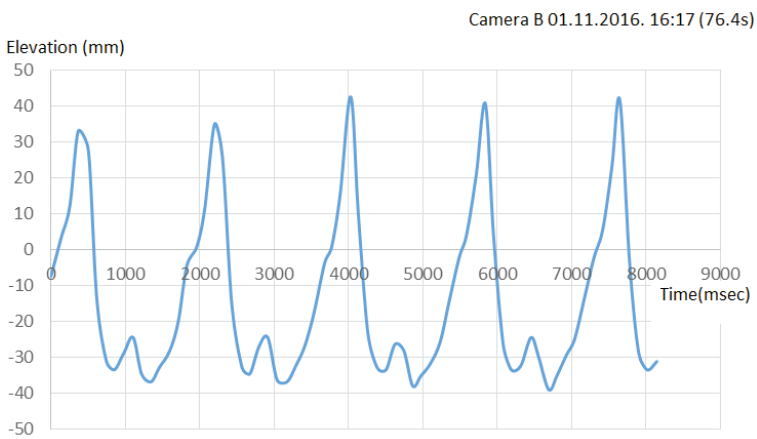

Fig. 7. Example of water wave time domain segment in measurement session, Camera B 16:17 01.11.2016.

To obtain the spectrum of normalized amplitude $A(m)$ of discrete sine wave m frequency $f(m)$, we used expression (10). To perform FFT, the number of analysing

function initial values has to be power of 2 (two) (16, 64, 128, 256, ...) to the argument, whose step must be constant (in practice, the number of initial values 1024 is used).

$$A(k) = \frac{IMABS\left(supplied\ complex\ variable(k)\right)}{512}, \tag{10}$$

where $$f(k) = k \cdot \frac{1}{T}. \tag{11}$$

The phase shift angle radians of oscillation frequency component θ (*k)* are available from the expression:

$$\theta(k) = IMARGUMENT\left(supplied\ complex\ variable(k)\right) \tag{12}$$

Thus, we have a visible picture of the constituent components of the oscillation (the amplitude and frequency known) (Fig. 8).

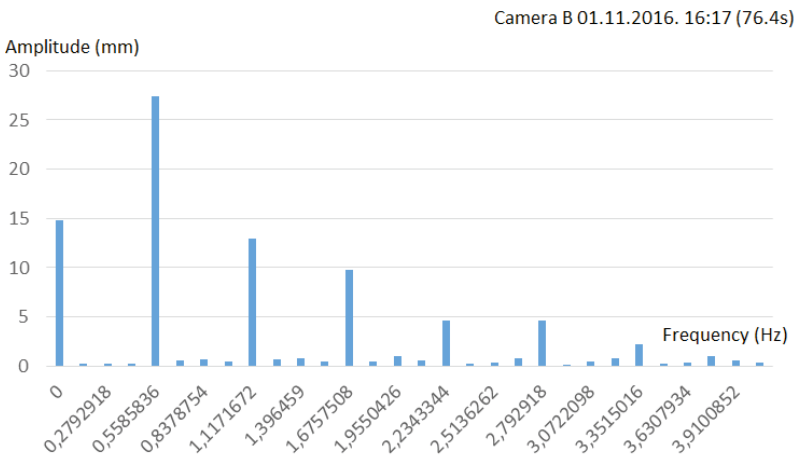

Fig. 8. Harmonic amplitude spectra after discrete Fourier transformation.

Using linear wave theory basic equation [4, p.408] we can calculate the average energy and power of each frequency *f(k)* component (harmonic) in this time segment:

$$E(k) = E_k(k) + E_p(k) = \frac{\rho g A^2(k)}{2} \tag{13}$$

and $$N(k) = E(k) \cdot C(k) = \frac{\rho g^2 A^2(k)}{4\pi f(k)}, \tag{14}$$

where k – discrete sine wave frequency number;
$A(k)$ – wave k-harmonic amplitude;
$f(k)$ – wave k-harmonic frequency;
ρ – water density;

g – gravitational constant;
Ek(k) – overage wave *k*- frequency harmonic kinetic energy*;*
Ep(k) – overage wave *k*- frequency harmonic potential energy*;*
E(k) – overage wave k- frequency harmonic energy*;*
N(k) – overage wave k- frequency harmonic power.

The last expression is applicable when for determination of the wavelength λ and the wave phase velocity C we can use the deep-water wave regularities (15,16), [2]:

$$\lambda = \lambda_0 = \frac{g \cdot T^2}{2\pi}, \tag{15}$$

$$C = C_0 = \frac{\lambda_0}{T} = \frac{g \cdot T}{2\pi}, \tag{16}$$

where λ_0 – wavelength in deep water;
C_0 – wave phase speed in deep water;
h – the water depth.

That is true if the conditions are met $h \geq \frac{\lambda_0}{4}$. (17)

If the condition is not met and $h < \frac{\lambda_0}{4}$, (18)

then assuming that there is not force of a deep-sea formula because although the wave height changes can be measured, the wave phase velocity C changes and should be calculated using equation (19) and for wave power calculation a correction $tanh\ (kh)$ should be applied for waveform at transition depth [2, p. 4]

$$C = C0\ \cdot tanh\ (lh), \tag{19}$$

where

l – wave number: $l\ = \frac{2\pi}{\lambda}$. (20)

An intermediate water wave length is

$$\lambda = C \cdot T = \frac{gT^2}{2\pi} \cdot tanh\left(\frac{2\pi h}{\lambda}\right). \tag{21}$$

It means, we have a transcendental equation (21), which is the reason why in practice for the adjustment we used graphics techniques [3, Fig. 2.2], which reflect the relative wave parameters $\frac{C}{C0}$ and $\frac{\lambda}{\lambda_0}$ as a function of depth and conditional deep-water wavelength relationship $\frac{h}{\lambda_0}$.

9. ENERGY SPECTRUM

Expression (14) allows getting an idea of the aggregate wave power (22) discrete frequency distribution (Fig. 9).

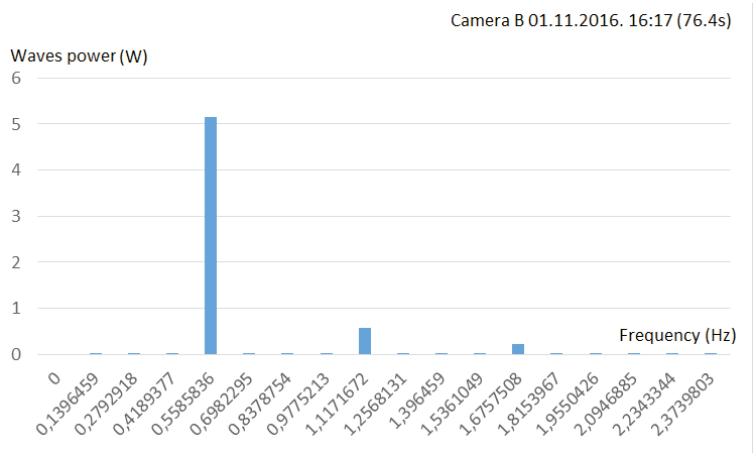

Fig. 9. Wave kinetic energy and average power frequency spectrum.

The total wave mean power N_{sum} of the plane wave, which is fitted with a laser measure gauge, is calculated as a sum of wave harmonic powers:

$$N_{sum} = \sum_{k=1}^{k_{sum}} N(k), \tag{22}$$

where k – wave harmonic number;

k_{sum} – upper frequency number value of wave harmonic sum range.

Figure 9 shows that to get wave power evaluation it is not necessary to sum all $j_{max}/2$ frequency harmonic powers. For present wave flume application above 2.8 Hz frequency power sum increase is practically zero (less than 0.2 %). Therefore, we can define wave harmonic frequency number limit or sum number range k_{sum}=20 (f(20)=2.8Hz).

10. THE SENSOR LOCATION

Locating wave environment “laser meter”, which can carry out the measurements and measure the oscillation amplitude and power management, should be based on a few considerations:

1. All of the aforementioned considerations are partly based on the assumption that the wave propagation direction is known because without additional conditions the practical wave propagation direction of point sensors cannot be determined. Conclusion – Lasers should be deployed in pairs. This theoretically makes it possible to experimentally determine the direction of wave propagation and wave phase speed, which is necessary for the calculation of wave power.

2. If foreign objects are inserted into the wave path dynamic system as a component, for example, with the object of wave energy absorption and conversion to another form of energy, in order to evaluate these devices it is necessary to obtain data on what part of the wave energy is consumed/ stifled. Conclusion – one detector should be placed in front of the equipment and the other – behind it.
3. Any foreign body will reflect part of the wave energy. This process affects the transformed energy balance / ratio. If this process is going to control the open water area, the receiver should be installed at a distance of two meters. A single detector and a fixed control measurement session without a receiver would suffice in a wave bath.

11. TESTING

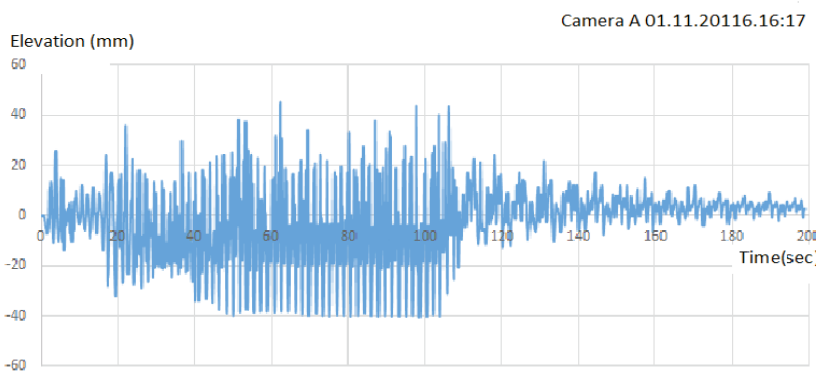

Fig. 10. Waves in a "no object" wave tank 1.95 m away from the wave generator.

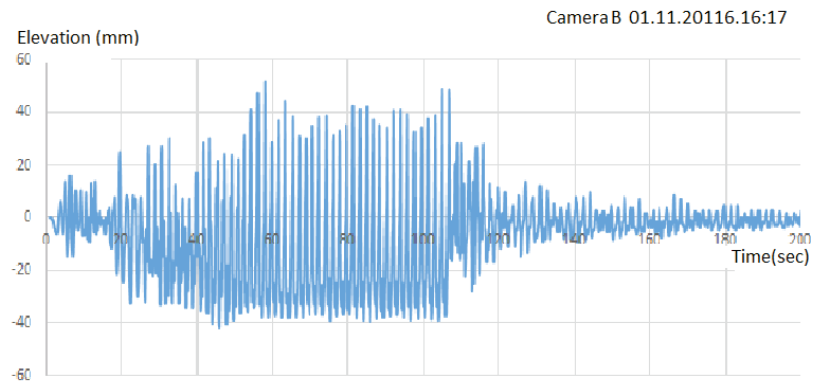

Fig. 11. Waves in a "no object" wave tank 3 m away from the A sensor and 1.98 m from the wave absorber.

On the basis of these considerations, in a wave bath 3 m away from each other, on both sides of the potential wave converter, 1.95 m away from the wave generator and 1.97 m from the wave absorber, we installed two calibrated measuring detectors (A, B). To test the wave tank unit, as regards to converter measurement, a test session without a converter was initiated (in a wave tank containing no alien object). The corresponding measurements are shown in Figs. 10 and 11.

12. CONCLUSIONS

The developed method allows for automated and efficient recording of wave surface elevation time function characterising data and saves them for further processing.

It allows keeping records of wave energy, power and determination of the changes between certain measure wave planes.

The chosen two laser measure configuration allows the receiver – wave tank system – to detect wave phenomena, such as resonance, standing waves, wave absorption, reflection, dispersion, and refraction.

Addressing the fluid wave energy receiver absorption determination, the project "Operation Research of a Twisting and Rotating Wave Energy Conversion Plant" within the framework of the solution chosen has been practically implemented (equipment and software have been developed for necessary measurements) and tested in real experimental conditions.

REFERENCES

1. Cimbala, J.M. (2010). *Fourier Transforms, DFTs, and FFTs*. Pensilvania, US: Penn State University. Available at http://www.mne.psu.edu/cimbala/me345/Lectures/Fourier_Transforms_DFTs_FFTs.pdf
2. Secretariat of the World Meteorological Organization. (1998). *Guide to Wave Analysis and Forecasting* (2nd ed.). Geneva, Switzerland, WMO-No. 702. Available at https://www.wmo.int/pages/prog/amp/mmop/documents/WMO%20No%20702/WMO702.pdf.
3. McCormic, M.E. (1981). *Ocean Vawe Energy Conversion*. New York, US: Wiley.
4. Twidell J., & Weir, T. (2006) *Renewable Energy Resources* (2nd ed.). London, UK: Taylor & Francis.

JAUDAS MĒRĪŠANA VIĻŅU ENERĢIJAS PĀRVEIDOTĀJU EFEKTIVITĀTES NOTEIKŠANAI

J. Beriņš, J. Beriņš, A. Kalnačs

K o p s a v i l k u m s

Raksts ir veltīts ūdens gravitācijas viļņu virsmas svārstību alternatīvas mērīšanas budžeta iekārtas tehniskā risinājuma un šo svārstību jaudas aprēķina teorētiskajam pamatojumam. Šis risinājums ietver tādas tehnoloģijas kā lāzera stars, WEB-kameras attēla ciparu apstrāde, neregulāros intervālos definēta funkcijas interpolācija, diskrētā Furjē transformācija svārstību harmoniku amplitūdu un jaudu frekvenču spektra aprēķināšanai.

12.04.2017.